Biophysical Journal Volume 99 December 2010 3951–3958

Nanotribology Results Show that DNA Forms a Mechanically Resistant 2D Network in Metaphase Chromatin Plates

Isaac Gállego,[†] Gerard Oncins,[‡] Xavier Sisquella,[§] Xavier Fernàndez-Busquets,[¶] and Joan-Ramon Daban[†*]
[†]Departament de Bioquímica i Biologia Molecular, Facultat de Biociències, Universitat Autònoma de Barcelona, Bellaterra, Spain; [‡]Scientific-Technical Services, Nanometric Techniques Unit, University of Barcelona, Barcelona, Spain; [§]Plataforma de Nanotecnologia, Parc Científic de Barcelona, Barcelona, Spain; and [¶]Grup de Nanobioenginyeria, Institut de Bioenginyeria de Catalunya, and Biomolecular Interactions Team, Nanoscience and Nanotechnology Institute, University of Barcelona, Barcelona, Spain

ABSTRACT In a previous study, we found that metaphase chromosomes are formed by thin plates, and here we have applied atomic force microscopy (AFM) and friction force measurements at the nanoscale (nanotribology) to analyze the properties of these planar structures in aqueous media at room temperature. Our results show that high concentrations of NaCl and EDTA and extensive digestion with protease and nuclease enzymes cause plate denaturation. Nanotribology studies show that native plates under structuring conditions (5 mM Mg^{2+}) have a relatively high friction coefficient ($\mu \approx 0.3$), which is markedly reduced when high concentrations of NaCl or EDTA are added ($\mu \approx 0.1$). This lubricant effect can be interpreted considering the electrostatic repulsion between DNA phosphate groups and the AFM tip. Protease digestion increases the friction coefficient ($\mu \approx 0.5$), but the highest friction is observed when DNA is cleaved by micrococcal nuclease ($\mu \approx 0.9$), indicating that DNA is the main structural element of plates. Whereas nuclease-digested plates are irreversibly damaged after the friction measurement, native plates can absorb kinetic energy from the AFM tip without suffering any damage. These results suggest that plates are formed by a flexible and mechanically resistant two-dimensional network which allows the safe storage of DNA during mitosis.

INTRODUCTION

In mitotic chromosomes, each chromatid contains a single DNA molecule (1). Typical metaphase chromatids have a diameter of ~500 nm and a length of several micrometers (2). These short cylinders contain extremely long DNA molecules (2–10 cm in the case of human chromosomes). The small cross section (~2 nm) of the DNA molecules makes them easily fragmentable by relatively low stretching forces (~1 nN (3)). Since the pulling force exerted by the mitotic spindle for the separation of the sister chromatids in anaphase is also in the nN range (4), DNA has to be protected within chromosomes. The structure of chromosomes must be capable of avoiding any mechanical damage of DNA during cell division.

It is known that DNA associated with histone proteins is densely packaged in condensed chromosomes (5). The basic structure of chromatin consists of DNA coiled around histone octamers (6), giving rise to a nucleosome filament. The stretching force required for nucleosome unfolding and dissociation of histones is 20–40 pN (7–9). The nucleosome filament complemented with histone H1 can be further folded into the 30-nm chromatin fiber, which may have different compaction degrees (10–14). The pulling force required for the decondensation of the folded chromatin fiber is 4–6 pN (7,15). Current models for the metaphase chromosome consider the 30-nm chromatin fiber to be the starting element that is folded within the condensed chromatids to form larger structures such as loops (16), fiber networks (17), or fibers with larger diameters (18).

In contrast to these fibrillar models, we found, using electron microscopy, that metaphase chromosomes are formed by platelike structures (19). These results were obtained in the presence of cation concentrations approaching those found in chromosomes during mitosis (20). Chromatin fibers are only visible in metaphase chromosomes treated with buffers containing extremely low cation concentrations. In agreement with these observations, Eltsov et al. (21) have reported that the analysis of mitotic-cell cryosections does not support the existence of 30-nm chromatin fibers in condensed chromosomes. Our electron microscopy images showed that chromosome plates can form multilayered structures, and the height measurements indicated that each layer has a thickness of ~6 nm. These observations and further structural studies performed using atomic force microscopy (AFM) led us to suggest the thin-plate model for chromatin folding in metaphase chromosomes (22), which proposed that chromosomes are formed by many stacked plates oriented perpendicular to the chromatid axis. This model allows an easy physical explanation of the characteristic banding patterns of metaphase chromosomes obtained in cytogenetic studies (2,23). Recently, using electron tomography and polarizing microscopy, we found that nucleosomes are irregularly oriented in well-defined plates that occupy the entire volume of the chromatid (24).

AFM is a powerful tool for investigating biological samples due to its ability to obtain images in a liquid environment at controlled temperature, mimicking physiological conditions

Submitted July 6, 2010, and accepted for publication November 10, 2010.
*Correspondence: joanramon.daban@uab.es
Editor: David P. Millar.

0006-3495/10/12/3951/8 $2.00
doi: 10.1016/j.bpj.2010.11.015

(25,26). On the other hand, the use of AFM as a nanomechanical probe has led to the development of force spectroscopy, which provides quantitative information about elastic and plastic properties of the sample (27–29). We showed previously that the plates emanating from metaphase chromosomes can be imaged using AFM in aqueous solution (22), and we found that in the presence of 5–20 mM Mg^{2+} the Young's modulus of plates is ~0.2 GPa and the force required for plate penetration with the AFM tip is 4–6 nN. In this work, we used AFM techniques to investigate the mechanical stability of individual plates under different denaturing conditions. Plate denaturation in aqueous media was monitored in real time at room temperature. Furthermore, recent technical and theoretical developments (30–33) have led to an increased interest in using AFM to study friction forces at the nanoscale (nanotribology). This technique is extremely sensitive to structural changes in soft-matter planar structures (34–37). In life sciences, nanotribology has been very useful for investigating lipid bilayers (38,39). To obtain a more complete knowledge of the structural and mechanical properties of the metaphase plates, we used AFM to carry out quantitative friction force measurements of native plates and plates in the presence of protease and nuclease enzymes and other denaturing agents. Our results demonstrate that DNA in plates is organized as a 2D network with a mechanical strength that may explain the maintenance of genetic integrity during mitosis.

MATERIALS AND METHODS

Metaphase chromosome plates and enzymes

Chromosomes from HeLa Cells were prepared in a buffer containing 15 mM triethanolamine-HCl (pH 7.5), 20 mM NaCl, 80 mM KCl, 0.2 mM spermine, 0.5 mM spermidine, 2 mM EDTA, and 0.5 mM EGTA, and purified on sucrose step gradients in accordance with previously described procedures (19). The gradients contained four layers of sucrose (30, 40, 50, and 60%) in 5 mM Pipes (pH 7.2), 5 mM NaCl, and 5 mM $MgCl_2$. Chromosomes were collected from the 40–50% and 50–60% interphases and finally where extensively dialyzed against the same buffer used in the gradient but without sucrose (in some experiments, this buffer contained, in addition, 1 mM EGTA; see below). Finally, the suspension of chromosomes was passed several times through a 22-gauge syringe needle to favor the emanation of plates from the chromatids (22). Trypsin and micrococcal nuclease were obtained from Sigma (St Louis, MO) and pronase from Roche (Penzberg, Germany).

AFM

For the visualization of plate denaturation, a 10-μL drop of the sample prepared as described above was adsorbed on freshly cleaved mica for 5 min and washed with 2–3 mL of 5 mM Pipes (pH 7.2), 5 mM NaCl, and 5 mM $MgCl_2$. In some experiments (Fig. 1, *a* and *b*), this solution contained 1 mM EGTA in addition. Before use, the sheets (3 × 3 mm) of mica (grade V1; Ted Pella, Redding, CA) were glued on top of a Teflon disc (9 mm in diameter). The different denaturing agents were added carefully (using a long micropipette tip) to the sample during AFM scanning of the surface. Imaging in the tapping mode was performed with an MFP-3D-BIO microscope (Asylum Research, Santa Barbara, CA). Images were generally obtained using silicon nitride V-shaped OMCL-TR400PSA cantilevers 200 μm long (nominal spring constant 0.02 N/m; Olympus, Tokyo, Japan),

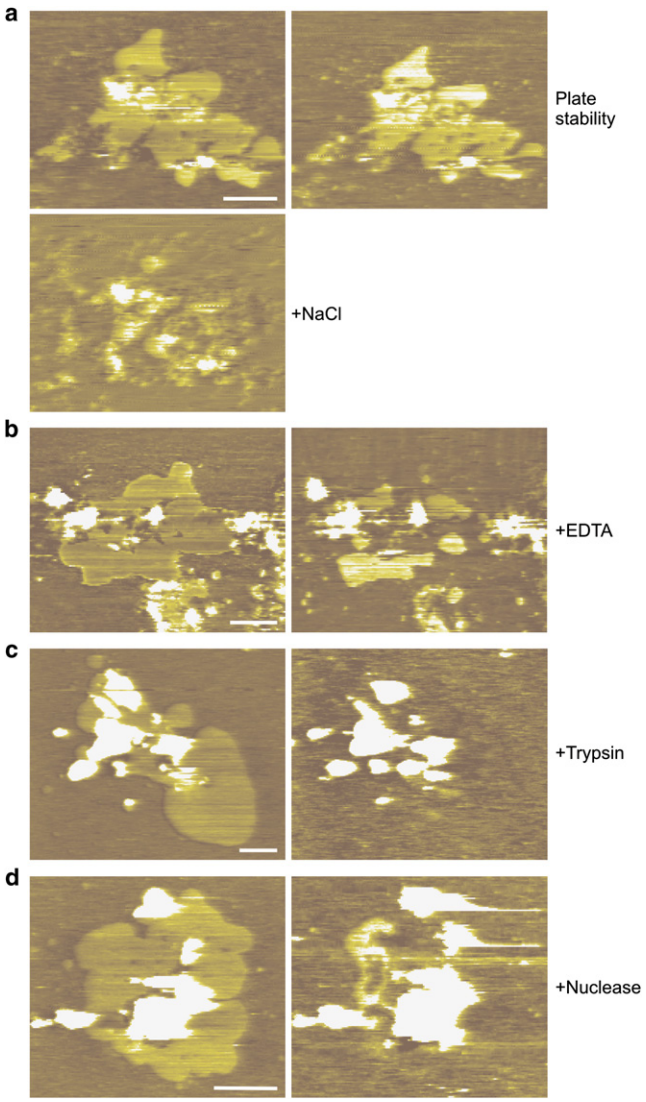

FIGURE 1 Direct AFM visualization of plate denaturation. (*a*) Two consecutive images of a plate before the addition of a concentrated solution of NaCl (final concentration ~1.3 M). The image of the denatured structure (*lower*) was obtained 43 min after the addition of NaCl. (*b*) The image at *right* was obtained 13 min after the addition of a concentrated solution of EDTA (final concentration ~6 mM). (*c*) Plates were completely denatured (see image at *right*) 53 min after the addition of trypsin (final concentration ~0.7 mg/mL). (*d*) The image at *right* was obtained 5 min after the addition of micrococcal nuclease (final concentration ~42 units/mL). In all images the plates show their characteristic smooth surface; the large amorphous aggregates are seen as intense white spots. Scale bars, 500 nm (*a*, *b*, and *d*) and 200 nm (*c*).

but the images corresponding to EDTA denaturation experiments (Fig. 1 *b*) were obtained with cantilevers 100 μm long (nominal spring constant 0.08 N/m). Frequency was set 5–10% lower than resonance (~13 kHz), with a free amplitude of 1 V; the set point was kept 20% below the free amplitude. Images were obtained at room temperature.

Nanotribology

For the friction measurements, 120 μL of the sample was adsorbed on freshly cleaved mica (grade V1; discs 9.9 mm in diameter glued to Teflon)

for 5 min and then washed with a solution containing 5 mM Pipes (pH 7.2), 5 mM NaCl, and 5 mM $MgCl_2$, and the indicated concentrations of denaturing agents. In the experiments with proteases and micrococcal nuclease, the samples contained, in addition, 1 mM Ca^{2+}. In some experiments (see Results), the denaturing agents were added directly to the sample with the AFM tip in contact with the liquid. Friction analysis and imaging were performed with a Dimension-3100 microscope (Veeco, Santa Barbara, CA) attached to a Nanoscope-IV controller in contact mode. Depending on the range of accessible vertical forces, we used V-shaped silicon nitride cantilevers with a nominal spring constant of 0.08 N/m (OMCL-TR400PSA, Olympus) or 0.32 N/m (DNP-C, Veeco). Force curves (i.e., vertical deflection of the cantilever-versus-piezo displacement) were obtained before acquiring topographic images; this allowed us to apply the minimum vertical force on the surface to avoid sample damage. Measurements were performed at room temperature. After aligning the laser with the cantilever immersed in the aqueous solution, the system was left to thermally equilibrate for ~30 min. To avoid changes of the photodiode sensitivity, the tip was rinsed with the appropriate buffer without being removed from the AFM holder. After the addition of concentrated solutions of NaCl and EDTA, there was a 15-min wait for cantilever equilibration before the beginning of the friction measurement.

Vertical spring constants of individual cantilevers were calibrated using the thermal noise method (40). These measurements were performed with an MFP-1D atomic force microscope (Asylum Research). To obtain quantitative friction values, the lateral force calibration (41) was performed using a wedge-shaped silicon oxide calibration grating (TGG01, MikroMasch, Wilsonville, OR). Raw data analysis was performed with MATLAB (The MathWorks, Natick, MA) scripts provided by R. Carpick's laboratory (42); the scripts were used to generate friction-versus-load data sets (i.e., plots of lateral force versus vertical force) from Nanoscope files. For friction-versus-load measurements an ascending sawtooth waveform from an external function generator (Agilent, Palo Alto, CA) was subtracted from the vertical photodetector signal obtained through the breakout box of the microscope (Veeco) using a home-made card. The resulting voltage was used as an input signal for the feedback control to maintain a steadily increasing normal force over the course of a friction-versus-load experiment. The scanned area was set to 300 nm at 6.1 Hz, with 512 lines and 512 pixels per line. As a result, a whole friction-versus-load curve ranging from low loads to high loads was obtained every 84 s. We chose to ramp the load from low to high values because we wanted to study the behavior of deposited plates as an increasing vertical force was applied.

RESULTS

Direct observation of denaturation of individual plates caused by changing ionic conditions and by digestion with protease and nuclease enzymes

We have previously shown (22) that plates from metaphase chromosomes can be imaged using AFM in aqueous media containing the structuring cation Mg^{2+} (5–30 mM). In the AFM images, plates show a smooth surface and are clearly distinguishable from the amorphous aggregates that are also present in many preparations. Under the AFM imaging conditions (see Methods) used in the experiments shown in Fig. 1, native plates in 5 mM Mg^{2+} are stable structures that can be imaged repeatedly without changing their appearance, but the addition of a concentrated solution of NaCl causes them to unfold (Fig. 1 *a*). This denaturation is presumably due to the dissociation of histones that occurs at a high ionic strength (43,44). On the other hand, the addition of EDTA also causes the denaturation of the plates (Fig. 1 *b*). In this case, the removal of the Mg^{2+} ions produced by the divalent cation chelator EDTA is probably responsible for the observed unfolding.

Fig. 1 *c* shows the effect of trypsin digestion on the structure of the plates surrounding the big aggregates, which are seen as intense white spots in the images. It can be observed that individual plates become disassembled upon trypsin digestion. Unfortunately, AFM imaging in aqueous media does not allow the visualization of the structural details of the resulting unfolded material. Micrococcal nuclease also causes complete disassembly of plates (Fig. 1 *d*). Therefore, it can be concluded that the enzymatic hydrolysis of proteins and DNA has a dramatic effect on the structure and mechanical stability of plates from metaphase chromosomes.

Frictional properties of native plates

Fig. 2 *a* shows the results of a typical friction experiment corresponding to plates under structuring conditions (5 mM Mg^{2+}). It can be seen that the experimental friction-versus-vertical force curve shown in this figure has three different regions. In region *A* (Fig. 2 *a*, *center*) the friction force is negligible and independent of the vertical force applied to the plate. As in the case of lipid bilayers (39), this lubricant behavior can be interpreted as a consequence of the repulsive electrostatic interaction between the plate surface and the tip. It is known that the DNA phosphate groups in the external surface of nucleosomes are not neutralized by histone positive charges (6,45). Thus, presumably due to the phosphate groups of DNA, there is a high density of negative charges in the plates that can produce a significant repulsion of the silicon nitride tip, which is also negatively charged (46). The discontinuity in region *B* is produced when the applied vertical force is high enough for the AFM tip to penetrate the plate surface. In the third region (region *C*) the friction force increases with the vertical force applied to the plate, giving rise to a significant friction coefficient (μ = friction force/vertical force (33)). We have performed equivalent measurements in many different experiments, and our results show that the friction coefficient of plates in the presence of structuring ionic conditions is 0.28 ± 0.09 (see Table 1). This value is significantly higher than the friction coefficient observed for the mica surface with the same tip under the same ionic conditions ($\mu = 0.18 \pm 0.09$, $n = 26$), indicating that after the tip penetration into the plate, the material of the plate is responsible for the observed friction force. This behavior was not observed in lipid bilayers (39); in this case, the AFM tip can actually break the bilayer, and the friction force is dominantly caused by the direct contact between the tip and the mica surface. Thus, according to the basic tribology theory (32–34), our results can be interpreted considering that native plates under structuring ionic conditions can absorb a significant amount of the

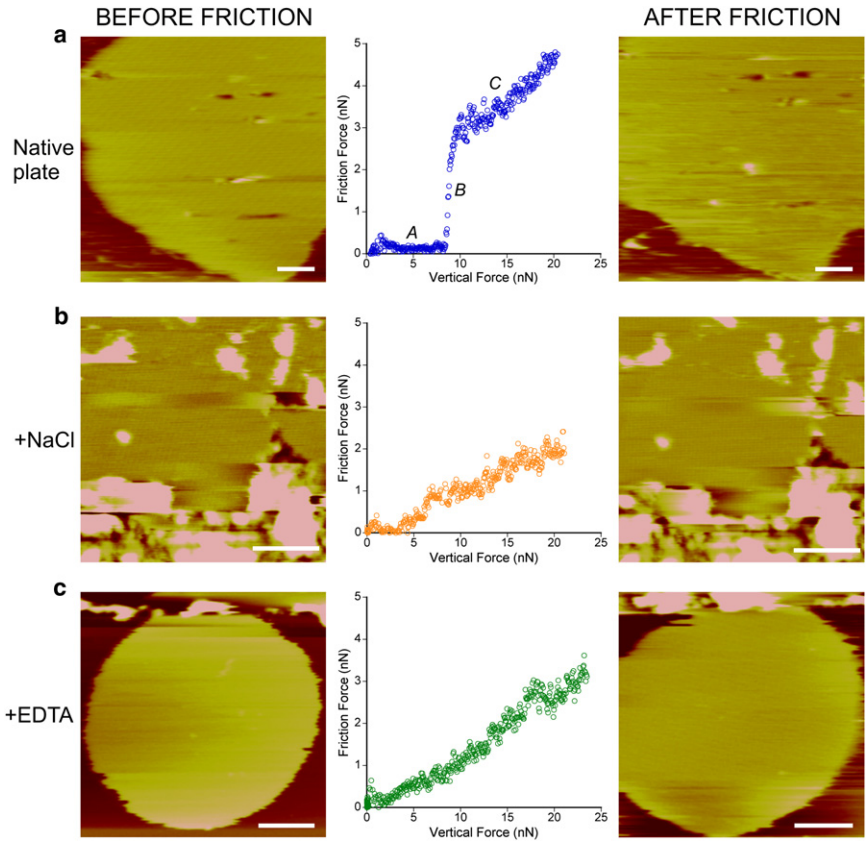

FIGURE 2 Nanotribology analysis of metaphase chromosome plates in the presence of NaCl and EDTA. (*a*) Images corresponding to a native plate before and after the measurement that produced the friction-versus-vertical force curve shown in this figure. Images of plates treated with ~2.9 M NaCl (*b*) and ~0.3 M EDTA (*c*) before and after the friction measurement that produced the curves shown in these figures. Scale bars, 250 nm.

translational kinetic energy from the AFM tip. Since plates are not damaged by scanning of regions of ~300 × 300 nm (not involving the edge) performed in the friction measurement (see example in Fig. 2 *a*, *right*), our results indicate that the structure of the plate is flexible and can return to its original conformation after the dissipation of the energy absorbed during the friction measurement.

Changes of the frictional properties of plates produced by high concentrations of NaCl and EDTA

In the presence of a high concentration of NaCl, the friction-versus-vertical force curve of the plates (Fig. 2 *b*) is very different from that observed under typical structuring conditions (Fig. 2 *a*). The discontinuity in the intermediate region is less apparent than that observed in native plates, and the friction coefficient observed in the presence of NaCl is smaller ($\mu = 0.05 \pm 0.02$; see Table 1). The dissociation of histones produced by high salt concentrations (histones are progressively released from 0.5 to 2.0 M NaCl (43,44)) increases the negative charge of the plate surface, but the screening effect of the Na^+ ions simultaneously reduces the repulsive force between the plate and the tip. Nevertheless, according to experimental results showing that high concentrations of NaCl produce a clear lubricant effect, it seems that under these conditions, the resultant repulsion between the plate surface and the tip is higher than that observed in the typical structuring ionic conditions.

The friction-versus-vertical force curves obtained in the presence of EDTA (Fig. 2 *c*) also indicate a low friction coefficient ($\mu = 0.12 \pm 0.04$; see Table 1) in comparison to native plates. The removal of Mg^{2+} cations from the plates produced by the relatively high concentration of EDTA (~0.3 M) used in these experiments is presumably responsible for a higher repulsion between the tip and the plate surface, leading to a significant decrease in the friction force. In addition, since we have used the disodium salt of EDTA, the Na^+ (~0.6 M) dissociated from EDTA can produce a screening of the negative charge of the tip and the phosphate groups, and probably a partial dissociation of histones, which may also contribute to some extent to the observed changes in the frictional properties of the plates.

Nuclease and protease digestion causes great changes in the frictional properties of the plates

Treatment of the plates with micrococcal nuclease and with a broad-spectrum protease (pronase) gives rise to a significant increase in the slope of the third region of the

TABLE 1 Friction coefficients of metaphase chromosome plates in the presence of diverse denaturing agents

Treatment*		$\mu^{\dagger}$
Native conditions		0.28 ± 0.09 ($n = 106$)
NaCl[‡]		0.05 ± 0.02 ($n = 22$)
EDTA[§]		0.12 ± 0.04 ($n = 37$)
Pronase[¶]	1/2	0.55 ± 0.06 ($n = 7$)
	1/5	0.49 ± 0.09 ($n = 14$)
	1/10	0.29 ± 0.12 ($n = 12$)
	1/20	0.26 ± 0.09 ($n = 33$)
	1/40	0.30 ± 0.11 ($n = 26$)
Nuclease[‖]	1/10	0.75 ± 0.09 ($n = 6$)
	1/40	0.91 ± 0.08 ($n = 4$)
	1/100	1.19 ± 0.24 ($n = 6$)
	1/500	0.56 ± 0.20 ($n = 10$)
	1/850	0.16 ± 0.05 ($n = 7$)
	1/5000	0.30 ± 0.04 ($n = 4$)

*All measurements were performed in aqueous solutions containing 5 mM Na^+ and 5 mM Mg^{2+} and the indicated denaturing agents.

[†]Values listed correspond to the mean ± SD obtained from the indicated number (n) of independent measurements obtained from different plates.

[‡]Concentrated solution of NaCl was added directly to the sample in the microscope to a final concentration of ~2.5 M.

[§]EDTA was also added directly to the sample to a final concentration of ~0.3 M.

[¶]Sample adsorbed on mica was treated with the indicated dilutions of a concentrated solution of pronase (~1 mg/mL).

[‖]Same procedure used for treatment with micrococcal nuclease as for pronase, with dilutions of concentrated solution (~126 units/mL) indicated.

friction-versus-vertical force curves (Fig. 3 and Table 1). The friction coefficient calculated from the curves corresponding to plates digested with pronase is twofold higher than that observed for native plates under the same structuring ionic conditions. A much higher increase of the friction coefficient is observed in the plates treated with micrococcal nuclease. Using intermediate dilutions of nuclease (see Table 1), the observed friction coefficient is approximately fourfold higher than that found for native plates. Furthermore, after the friction measurements of plates treated with nuclease, the region scanned by the AFM tip became completely disassembled (Fig. 3 *a*, *right*; note the clear hole of ~300 × 300 nm produced by the AFM tip). This complete denaturation of the scanned region was observed with nuclease dilutions up to 1/40. More diluted nuclease solutions generally did not cause any apparent damage of the plate but yielded very high friction coefficients ($\mu = 1.19 \pm 0.24$ using a nuclease dilution of 1/100; see Table 1).

These results can be interpreted considering that both protease and nuclease produce denaturation of the plate structure. The resulting denatured plates absorb more energy from the scanning tip than the native plates, and consequently, there is an increase of the friction coefficient. Friction increases with nuclease concentration up to a maximum value observed with a nuclease dilution of 1/100; higher nuclease concentrations produce relatively lower friction (see Table 1). This suggests that above a certain level of DNA breakage, the cohesion of the network within the plate is severely damaged, causing a decrease in the observed friction force. Furthermore, the irreversible structural changes observed under these digestion conditions indicate that in these samples, part of the energy absorbed from the tip is used for a permanent plastic deformation of the scanned region.

Our findings, which show that 1), the highest increase in the friction coefficient is observed in plates treated with nuclease; and 2), plates are severely damaged by the AFM tip during the friction measurement performed after nuclease digestion (but not after pronase digestion), indicate that DNA is the main structural element of the plates. The cleavage of DNA produced by nuclease leads to a dramatic change of the mechanical properties of the plates that cannot be achieved either by protein digestion or by treatment with high concentrations of NaCl and EDTA.

DISCUSSION

The chromosomes used in our study were prepared in the presence of polyamines at a concentration (0.2 mM spermine and 0.5 mM spermidine) similar to that currently used for the preparation of nucleosomes and chromatin (47). For the preparation of plates, chromosomes were further purified and extensively dialyzed in buffers containing 5 mM Mg^{2+}. We have previously shown, using different microscopy techniques, that plates are the dominant component of the compact chromatids obtained in the presence of polyamines or Mg^{2+} (19,22,24). In this study, neither chromosomes nor plates were fixed with glutaraldehyde or organic media. We applied AFM imaging and lateral force spectroscopy to analyze the mechanical properties of individual plates from metaphase chromosomes in aqueous media. Under the scanning conditions used in our imaging experiments, we observed that high concentrations of NaCl and EDTA produce plate unfolding. This behavior is consistent with the well-known properties of chromatin considered above. The decrease of the friction coefficient of plates in the presence of NaCl and EDTA can be interpreted considering the increase of the net negative charge of the plate surface produced by these treatments. These results do not rule out the possibility that plates could be produced artifactually during chromosome preparation, but they indicate that plates show the typical behavior of structures formed by condensed chromatin.

Under the structuring ionic conditions used in this work, the plates are mechanically stable. Native plates show a relatively high friction coefficient, but there is no sign of any structural alteration of native plates in 5 mM Mg^{2+} after the scanning performed in the friction measurements. Protease digestion causes a significant increase of the friction coefficient, but the highest friction is produced by nuclease digestion. Even diluted nuclease solutions yield high friction coefficients, indicating that DNA cleavage leads to a severe alteration of the plate, which may absorb

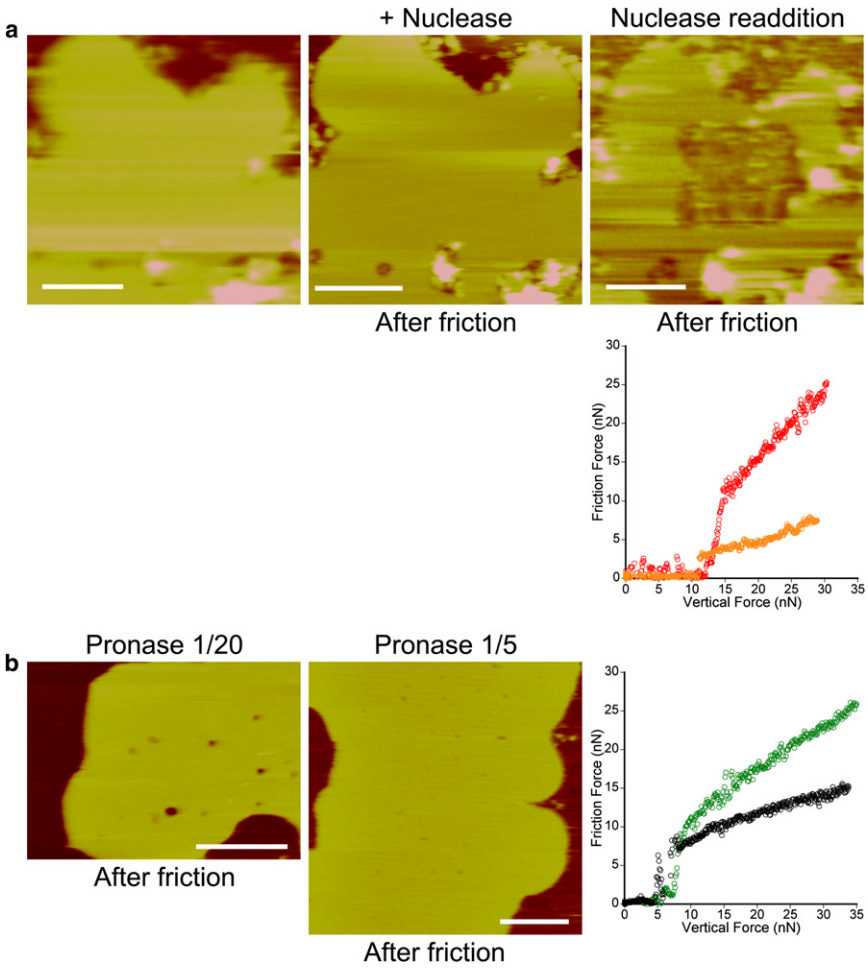

FIGURE 3 Nanotribology analysis of metaphase chromosome plates treated with nuclease and protease enzymes. (*a*, *left* and *middle*) The plate was treated with micrococcal nuclease (~6 units/mL) and imaged (*middle*) after the measurement that produced the orange curve in the friction-versus-vertical force plot (*inset*). After the readdition of nuclease (final concentration ~13 units/mL), the *red* curve was obtained; the image obtained after this friction measurement is shown at *right*. (*b*) Images corresponding to plates treated with 1/20 and 1/5 dilutions of a concentrated solution of pronase (~1 mg/mL) after the friction measurements that produced the *black* and *green* curves, respectively (*inset*). Scale bars, 250 nm (*a*) and 500 nm (*b*).

more energy from the scanning tip than the plates digested with protease. The absence of any apparent alteration in the structure of native plates does not exclude the possibility that DNA may be broken during nanotribology experiments. However, since the cleavage of DNA by nuclease produces a high increase in the friction coefficient in comparison to native plates, presumably in undigested plates the level of DNA breakage is very low. In addition, plates treated with higher concentrations of nuclease are irreversibly denatured after the friction measurement. Thus, it can be concluded from these results that DNA is the main element responsible for the mechanical strength of the plates. Micromechanical studies performed with whole chromosomes in aqueous solution treated with protease (48) and nuclease (17) enzymes also indicate that the mechanical integrity of mitotic chromosomes is mainly due to DNA.

In addition, as indicated in the Introduction, it has to be taken into account that individual DNA molecules can be broken with pulling forces of ~1 nN (3), but in nanotribology experiments, we applied higher lateral forces (up to ~5 nN) without producing any detectable damage to the undigested plates (Fig. 2 *a*). The observed relatively high friction coefficient of native plates indicates that the internal structure of the plates makes it possible for the energy absorbed from the AFM tip to dissipate without causing any apparent damage. The tip scanning causes reversible structural changes in the plate, presumably including a transient unfolding of nucleosomes. Furthermore, since the pulling force required for nucleosome disassembly is very small (see Introduction (7–9)), the scanning could even produce histone dissociation. In fact, many studies indicate that nucleosomes are dynamic structures that can adopt different conformations and may have different histone compositions (49,50). According to our results, after the passage of the tip, the original structure must be recovered. Early studies performed with purified DNA and histones (44,51,52) demonstrated that there are rapid spontaneous reactions for nucleosome reassociation and folding. These reactions have intermediates formed by partially assembled nucleosomes and nucleosomes containing excess histones, which could be transiently produced in the friction experiments. Therefore, we can conclude that DNA forms a 2D network in plates and that DNA is the fundamental element holding the structure together. Our findings also indicate that at the

same time, the dynamic mechanical properties of the entire planar structure protect DNA against breakage. Our results suggest that in native chromosomes the good flexibility and mechanical strength of the plates could be an effective mechanism to protect the integrity of whole genomic DNA during mitosis. In addition to the protection of the covalent bonds of DNA, the reversible recovery of plate structure observed after friction scanning with high lateral forces suggests that the good mechanical properties of the plates may contribute to maintenance of the whole chromosome structure during anaphase.

In this work, we have demonstrated that nanotribology, a technique originally devoted to the study of materials of technological interest, can be successfully applied to study very complex biomolecular structures such as metaphase chromatin plates. On the other hand, considering the great interest in nanostructures generated by taking advantage of the self-assembly properties of DNA (53–57), the good mechanical characteristics of the DNA-protein films studied in this work could be useful for future development of new biologically inspired materials.

Cell culture was performed in the Unitat de Cultius Cel·lulars (UAB).

This work was supported in part by grants BFU2005-3883 and BFU2008-04514-E (to J.R.D.) and BIO2008-01184 and CSD2006-00012 (to X.F.B.) from the Ministerio de Ciencia e Innovación, which included FEDER founds, and by grant 2009SGR-760 from the Generalitat de Catalunya (to X.F.B). I.G. was supported by a predoctoral fellowship from the Generalitat de Catalunya.

REFERENCES

1. Lander, E. S., L. M. Linton, …, M. J. Morgan. 2001. Initial sequencing and analysis of the human genome. *Nature.* 409:860–921.
2. Sumner, A. T. 2003. Chromosomes: Organization and Function. Blackwell Publishing, Oxford, United Kingdom.
3. Bustamante, C., S. B. Smith, …, D. Smith. 2000. Single-molecule studies of DNA mechanics. *Curr. Opin. Struct. Biol.* 10:279–285.
4. Nicklas, R. B. 1983. Measurements of the force produced by the mitotic spindle in anaphase. *J. Cell Biol.* 97:542–548.
5. Daban, J. R. 2000. Physical constraints in the condensation of eukaryotic chromosomes. Local concentration of DNA versus linear packing ratio in higher order chromatin structures. *Biochemistry.* 39: 3861–3866.
6. Luger, K., A. W. Mäder, …, T. J. Richmond. 1997. Crystal structure of the nucleosome core particle at 2.8 A resolution. *Nature.* 389:251–260.
7. Cui, Y., and C. Bustamante. 2000. Pulling a single chromatin fiber reveals the forces that maintain its higher-order structure. *Proc. Natl. Acad. Sci. USA.* 97:127–132.
8. Bennink, M. L., S. H. Leuba, …, J. Greve. 2001. Unfolding individual nucleosomes by stretching single chromatin fibers with optical tweezers. *Nat. Struct. Biol.* 8:606–610.
9. Brower-Toland, B. D., C. L. Smith, …, M. D. Wang. 2002. Mechanical disruption of individual nucleosomes reveals a reversible multistage release of DNA. *Proc. Natl. Acad. Sci. USA.* 99:1960–1965.
10. Daban, J. R. 2003. High concentration of DNA in condensed chromatin. *Biochem. Cell Biol.* 81:91–99.
11. Robinson, P. J. J., and D. Rhodes. 2006. Structure of the '30 nm' chromatin fibre: a key role for the linker histone. *Curr. Opin. Struct. Biol.* 16:336–343.
12. Wong, H., J. M. Victor, and J. Mozziconacci. 2007. An all-atom model of the chromatin fiber containing linker histones reveals a versatile structure tuned by the nucleosomal repeat length. *PLoS ONE.* 2:e877.
13. Grigoryev, S. A., G. Arya, …, T. Schlick. 2009. Evidence for heteromorphic chromatin fibers from analysis of nucleosome interactions. *Proc. Natl. Acad. Sci. USA.* 106:13317–13322.
14. Stehr, R., R. Schöpflin, …, G. Wedemann. 2010. Exploring the conformational space of chromatin fibers and their stability by numerical dynamic phase diagrams. *Biophys. J.* 98:1028–1037.
15. Kruithof, M., F. T. Chien, …, J. van Noort. 2009. Single-molecule force spectroscopy reveals a highly compliant helical folding for the 30-nm chromatin fiber. *Nat. Struct. Mol. Biol.* 16:534–540.
16. Saitoh, Y., and U. K. Laemmli. 1994. Metaphase chromosome structure: bands arise from a differential folding path of the highly AT-rich scaffold. *Cell.* 76:609–622.
17. Poirier, M. G., and J. F. Marko. 2002. Mitotic chromosomes are chromatin networks without a mechanically contiguous protein scaffold. *Proc. Natl. Acad. Sci. USA.* 99:15393–15397.
18. Strukov, Y. G., Y. Wang, and A. S. Belmont. 2003. Engineered chromosome regions with altered sequence composition demonstrate hierarchical large-scale folding within metaphase chromosomes. *J. Cell Biol.* 162:23–35.
19. Caravaca, J. M., S. Caño, …, J. R. Daban. 2005. Structural elements of bulk chromatin within metaphase chromosomes. *Chromosome Res.* 13:725–743.
20. Strick, R., P. L. Strissel, …, R. Levi-Setti. 2001. Cation-chromatin binding as shown by ion microscopy is essential for the structural integrity of chromosomes. *J. Cell Biol.* 155:899–910.
21. Eltsov, M., K. M. Maclellan, …, J. Dubochet. 2008. Analysis of cryo-electron microscopy images does not support the existence of 30-nm chromatin fibers in mitotic chromosomes in situ. *Proc. Natl. Acad. Sci. USA.* 105:19732–19737.
22. Gállego, I., P. Castro-Hartmann, …, J. R. Daban. 2009. Dense chromatin plates in metaphase chromosomes. *Eur. Biophys. J.* 38:503–522.
23. Shaffer, L. G., and N. Tommerup. 2005. An International System for Human Cytogenetic Nomenclature. Karger, Basel.
24. Castro-Hartmann, P., M. Milla, and J. R. Daban. 2010. Irregular orientation of nucleosomes in the well-defined chromatin plates of metaphase chromosomes. *Biochemistry.* 49:4043–4050.
25. Müller, D. J., and K. Anderson. 2002. Biomolecular imaging using atomic force microscopy. *Trends Biotechnol.* 20:S45–S49.
26. Murphy, M. F., M. J. Lalor, …, D. R. Burton. 2006. Comparative study of the conditions required to image live human epithelial and fibroblast cells using atomic force microscopy. *Microsc. Res. Tech.* 69:757–765.
27. Heinz, W. F., and J. H. Hoh. 1999. Spatially resolved force spectroscopy of biological surfaces using the atomic force microscope. *Trends Biotechnol.* 17:143–150.
28. Zlatanova, J., S. M. Lindsay, and S. H. Leuba. 2000. Single molecule force spectroscopy in biology using the atomic force microscope. *Prog. Biophys. Mol. Biol.* 74:37–61.
29. Cornish, P. V., and T. Ha. 2007. A survey of single-molecule techniques in chemical biology. *ACS Chem. Biol.* 2:53–61.
30. Park, J. Y., D. F. Ogletree, …, M. Salmeron. 2006. Electronic control of friction in silicon pn junctions. *Science.* 313:186.
31. Socoliuc, A., E. Gnecco, …, E. Meyer. 2006. Atomic-scale control of friction by actuation of nanometer-sized contacts. *Science.* 313: 207–210.
32. Cannara, R. J., M. J. Brukman, …, R. W. Carpick. 2007. Nanoscale friction varied by isotopic shifting of surface vibrational frequencies. *Science.* 318:780–783.
33. Mo, Y., K. T. Turner, and I. Szlufarska. 2009. Friction laws at the nanoscale. *Nature.* 457:1116–1119.
34. Salmeron, M. 2001. Generation of defects in model lubricant monolayers and their contribution to energy dissipation in friction. *Tribol. Lett.* 10:69–79.

35. Brukman, M. J., G. Oncins Marco, …, R. W. Carpick. 2006. Nanotribological properties of alkanephosphonic acid self-assembled monolayers on aluminum oxide: effects of fluorination and substrate crystallinity. *Langmuir.* 22:3988–3998.

36. Flater, E. E., W. R. Ashurst, and R. W. Carpick. 2007. Nanotribology of octadecyltrichlorosilane monolayers and silicon: self-mated versus unmated interfaces and local packing density effects. *Langmuir.* 23: 9242–9252.

37. Colburn, T. J., and G. J. Leggett. 2007. Influence of solvent environment and tip chemistry on the contact mechanics of tip-sample interactions in friction force microscopy of self-assembled monolayers of mercaptoundecanoic acid and dodecanethiol. *Langmuir.* 23: 4959–4964.

38. Grant, L. M., and F. Tiberg. 2002. Normal and lateral forces between lipid covered solids in solution: correlation with layer packing and structure. *Biophys. J.* 82:1373–1385.

39. Oncins, G., S. Garcia-Manyes, and F. Sanz. 2005. Study of frictional properties of a phospholipid bilayer in a liquid environment with lateral force microscopy as a function of NaCl concentration. *Langmuir.* 21:7373–7379.

40. Florin, E. L., M. Rief, …, H. E. Gaub. 1995. Sensing specific molecular interactions with the atomic force microscopy. *Biosens. Bioelectron.* 10:895–901.

41. Ogletree, D. F., R. W. Carpick, and M. Salmeron. 1996. Calibration of frictional forces in atomic force microscopy. *Rev. Sci. Instrum.* 67:3298–3306.

42. http://nanoprobenetwork.org/software-library/welcome-to-the-carpick-labs-software-toolbox.

43. Burton, D. R., M. J. Butler, …, I. O. Walker. 1978. The interaction of core histones with DNA: equilibrium binding studies. *Nucleic Acids Res.* 5:3643–3663.

44. Aragay, A. M., X. Fernàndez-Busquets, and J. R. Daban. 1991. Different mechanism for in vitro formation of nucleosome core particles. *Biochemistry.* 30:5022–5032.

45. Mirzabekov, A. D., and A. Rich. 1979. Asymmetric lateral distribution of unshielded phosphate groups in nucleosomal DNA and its role in DNA bending. *Proc. Natl. Acad. Sci. USA.* 76:1118–1121.

46. Butt, H. J. 1991. Measuring electrostatic, van der Waals, and hydration forces in electrolyte solutions with an atomic force microscope. *Biophys. J.* 60:1438–1444.

47. Kornberg, R. D., J. W. LaPointe, and Y. Lorch. 1989. Preparation of nucleosomes and chromatin. *Methods Enzymol.* 170:3–14.

48. Pope, L. H., C. Xiong, and J. F. Marko. 2006. Proteolysis of mitotic chromosomes induces gradual and anisotropic decondensation correlated with a reduction of elastic modulus and structural sensitivity to rarely cutting restriction enzymes. *Mol. Biol. Cell.* 17:104–113.

49. Lavelle, C., and A. Prunell. 2007. Chromatin polymorphism and the nucleosome superfamily: a genealogy. *Cell Cycle.* 6:2113–2119.

50. Zlatanova, J., T. C. Bishop, …, K. van Holde. 2009. The nucleosome family: dynamic and growing. *Structure.* 17:160–171.

51. Aragay, A. M., P. Diaz, and J. R. Daban. 1988. Association of nucleosome core particle DNA with different histone oligomers. Transfer of histones between DNA-(H2A,H2B) and DNA-(H3,H4) complexes. *J. Mol. Biol.* 204:141–154.

52. Samsó, M., and J. R. Daban. 1993. Unfolded structure and reactivity of nucleosome core DNA-histone H2A,H2B complexes in solution as studied by synchrotron radiation x-ray scattering. *Biochemistry.* 32:4609–4614.

53. Rothemund, P. W. K. 2006. Folding DNA to create nanoscale shapes and patterns. *Nature.* 440:297–302.

54. Nykypanchuk, D., M. M. Maye, …, O. Gang. 2008. DNA-guided crystallization of colloidal nanoparticles. *Nature.* 451:549–552.

55. Park, S. Y., A. K. R. Lytton-Jean, …, C. A. Mirkin. 2008. DNA-programmable nanoparticle crystallization. *Nature.* 451:553–556.

56. He, Y., T. Ye, …, C. Mao. 2008. Hierarchical self-assembly of DNA into symmetric supramolecular polyhedra. *Nature.* 452:198–201.

57. Douglas, S. M., H. Dietz, …, W. M. Shih. 2009. Self-assembly of DNA into nanoscale three-dimensional shapes. *Nature.* 459:414–418.